

Characterizing the Intrinsic Strength (Fatigue Threshold) of Natural Rubber/Butadiene Rubber Blends

REFERENCE: Robertson, C. G., Stoček, R., Kipscholl, C., and Mars, W. V., “Characterizing the Intrinsic Strength (Fatigue Threshold) of Natural Rubber/Butadiene Rubber Blends,” *Tire Science and Technology*, TSTCA, Vol. 47, No. 4, October–December 2019, pp. 292–307.

ABSTRACT: Tires require rubber compounds capable of enduring more than 10^8 deformation cycles without developing cracks. One strategy for evaluating candidate compounds is to measure the intrinsic strength, which is also known as the fatigue threshold or endurance limit. The intrinsic strength is the residual strength remaining in the material after the strength-enhancing effects of energy dissipation in crack tip fields are removed. If loads stay always below the intrinsic strength (taking proper account of the possibility that the intrinsic strength may degrade with aging), then cracks cannot grow. Using the cutting protocol proposed originally by Lake and Yeoh, as implemented on a commercial intrinsic strength analyzer, the intrinsic strength is determined for a series of carbon black (CB) reinforced blends of natural rubber (NR) and butadiene rubber (BR) typical of tire applications. The intrinsic strength benefits of the blends over the neat NR and BR compounds are only observed after aging at temperatures in the range from 50 to 70 °C, thus providing fresh insights into the widespread durability success of CB-filled NR/BR blends in tire sidewall compounds and commercial truck tire treads.

KEY WORDS: fatigue, crack growth resistance, durability, tire sidewall compounds, TBR tread compounds, rubber testing, intrinsic strength

Introduction

The strength of rubber depends on its chemical structure, as well as on the viscoelastic behavior occurring in crack near-tip fields [1,2]. Owing to viscoelastic energy dissipation, the total energy required to propagate a crack in rubber is usually significantly greater than the energy associated with the intrinsic strength of the molecular structure. Traditional testing methods that are used in the rubber industry to measure tear and crack growth properties make it very difficult to perform the detailed structure–property relationship studies that are necessary for rational design of improved compounds for demanding applications such as tires. Assigning clear responsibility for crack growth resistance to certain structural features of the compound is very difficult,

¹ Corresponding authors. Endurica LLC, 1219 West Main Cross Street, Suite 201, Findlay, Ohio 45840, USA. Email: cgrobertson@endurica.com; wvmars@endurica.com

² PRL Polymer Research Lab s.r.o., Nad Ovčírnou IV 3685, 760 01 Zlín, Czech Republic

³ Coesfeld GmbH & Co. KG, Tronjesträße 8, 44319 Dortmund, Germany

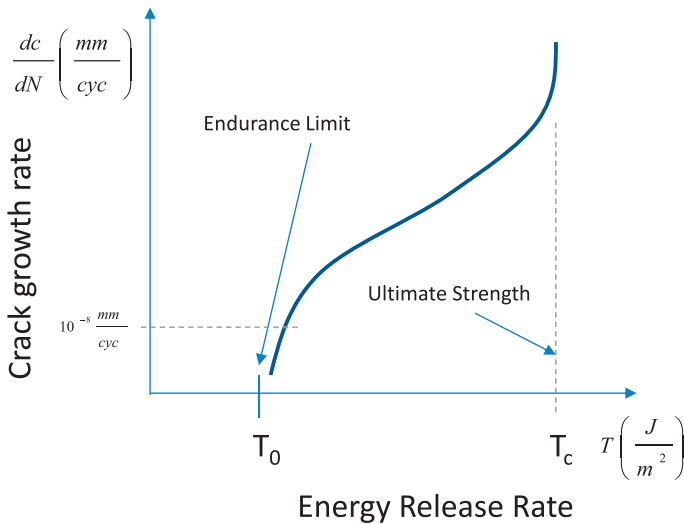


FIG. 1 — Diagram showing typical behavior for crack growth rate of rubber on a log–log plot versus energy release rate. The lower bound on the fatigue crack growth rate curve is the endurance limit, T_0 .

because these same material characteristics influence the hysteresis behavior of the rubber, which is a very large contributor to the bulk fracture response that is measured.

If a crack grows in a cross-linked polymer, it means at least that all polymer chains crossing the plane of the crack have ruptured, and there is a minimum energy requirement for this fracture. For a simple unfilled cross-linked elastomer, this minimum energy depends primarily on details of the polymer network, such as average molecular weight between cross-links, and on the weakest bond in the main polymer chain [3]. It is largely independent of time, temperature, and degree of swelling. It is therefore often called the intrinsic strength, since it reflects the polymer chemistry and network [4].

One practical reason for wanting to quantify the intrinsic strength (T_0) is that it marks the lower limit of the fatigue crack growth rate curve that is illustrated in Fig. 1 [5,6]. A crack operating at an energy release rate below the intrinsic strength can be projected to operate indefinitely without growing, since there is simply not enough energy supplied to break polymer chains at the crack tip [7]. Therefore, this endurance limit or mechanical fatigue limit is very useful in product design and in fatigue analysis [8].

At high values of energy release rate (T), also called tearing energy [9], the critical tearing energy (T_c)—sometimes called ultimate tear strength—is observed for an elastomer that marks the upper end of the fatigue crack growth response where catastrophic tearing occurs. Therefore, T_0 and T_c define the

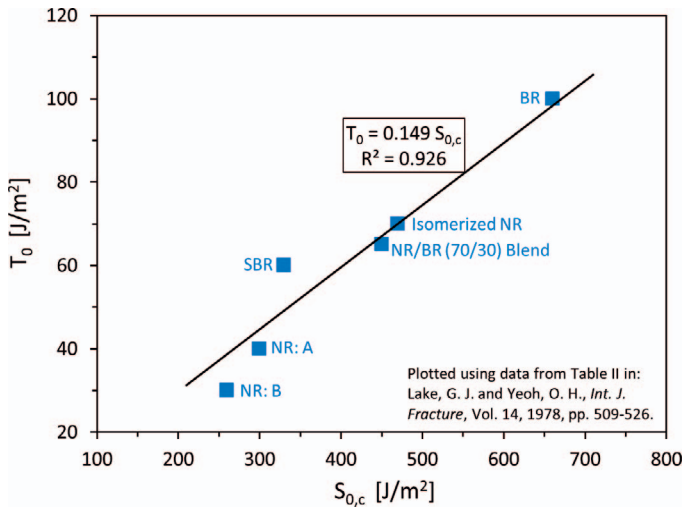


FIG. 2 — Correlation between intrinsic strength (T_0) (from lengthy fatigue crack growth measurements near the fatigue threshold) and intrinsic cutting energy ($S_{0,c}$) (from the cutting method) for various unfilled rubbers. The data plotted are from Table II of Lake and Yeoh [15]. See the cited reference for descriptions of the rubber materials evaluated.

window within which cracks grow due to the application of cyclic deformation. The crack growth behavior in this fatigue damage accumulation regime is affected by frequency, nature of the waveform (e.g., pulse versus sine wave), and maximum and minimum cyclic load limits [10–14]. There have not been enough detailed studies to know the effects of these testing variables on the fatigue threshold, T_0 .

The aim of this work is to determine the influence of thermal-oxidative aging on the intrinsic strength of compounds containing natural rubber, butadiene rubber, and their blends in model carbon black reinforced formulations that are representative of tire applications. The work uses a new commercial instrument and test procedure based on the theoretical background and cutting method of Lake and Yeoh [15] to evaluate the intrinsic strength as a function of polymer blend composition and aging temperature. An essential underpinning of the Lake and Yeoh approach is that the intrinsic cutting energy ($S_{0,c}$) determined from this method is correlated with T_0 measured from crack growth testing near the fatigue threshold (Fig. 2). It is necessary to evaluate very slow crack growth rates (10^{-8} to 10^{-9} mm/cycle) near the threshold in order to quantify the T_0 asymptote in Fig. 1, which can take several months at a typical frequency of 10 Hz. Therefore, the cutting procedure offers an effective laboratory testing alternative that can provide results within a few hours, by contrast.

TABLE 1 — Rubber Formulations.^a

| | NR | BR | NR/BR (75/25) | NR/BR (50/50) | Unfilled SBR Control |
|---------------------|-------------|-------------|------------------|------------------|-------------------------|
| NR | 100 | — | 75 | 50 | — |
| BR | — | 100 | 25 | 50 | — |
| SBR | — | — | — | — | 100 |
| Carbon black (N339) | 50 | 50 | 50 | 50 | — |
| Zinc oxide | 3 | 3 | 3 | 3 | 5 |
| Stearic acid | 1 | 1 | 1 | 1 | 2 |
| IPPD ^b | 1.5 | 1.5 | 1.5 | 1.5 | — |
| 6PPD ^c | — | — | — | — | 1 |
| CBS ^d | 2.5 | 2.5 | 2.5 | 2.5 | 1 |
| Sulfur | 1.7 | 1.7 | 1.7 | 1.7 | 1.75 |
| Cure temp. (°C) | 160 | 160 | 160 | 160 | 140 |
| Cure time (min) | t90 + 2 min | t90 + 2 min | t90 + 2 min | t90 + 2 min | 50 |

^aUnits are parts per hundred rubber unless otherwise indicated.

^b*N*-isopropyl-*N'*-phenyl-*p*-phenylenediamine.

^c*N*-(1,3-dimethylbutyl)-*N'*-phenyl-*p*-phenylenediamine.

^d*N*-cyclohexyl-2-benzothiazole sulfenamide.

Immiscible polymer blends do not generally have desirable mechanical properties. A notable exception is the phase-separated natural rubber/butadiene rubber (NR/BR) blend system reinforced with carbon black particles, which has such excellent durability that it is used in the sidewalls of nearly every automobile tire on the road and in many of the treads on truck and bus radial (TBR) tires. Despite progress throughout the years to understand the tear and fatigue behavior of this unique and important carbon black (CB)-filled rubber blend [16–21], there is no widely accepted fundamental conclusion about the origin of its exceptional durability characteristics in tire applications. This provides motivation for the present study.

Experimental Details

Polymers used in this study were natural rubber (SMR CV 60), high cis butadiene rubber (Buna CB 24 from Arlanxeo, Dormagen, Germany), and emulsion polymerized styrene-butadiene rubber (SBR 1500 from Trinseo, Schkopau, Germany). The reinforcing filler was N339 grade of carbon black. The rubber formulations are given in Table 1, where it can be observed that two NR/BR blends were included in this investigation: NR-rich 75/25 blend and a 50/50 blend. The other ingredients listed in Table 1 are standard rubber chemicals.

Rubber compounds were prepared in two mixing stages. For the first stage, all ingredients except *N*-cyclohexyl-2-benzothiazole sulfenamide (CBS) accelerator and sulfur were mixed for 5 minutes in an internal mixer (SYD-



FIG. 3 — Photograph of the Coesfeld Intrinsic Strength Analyzer.

2L from Everplast, Tainan City, Taiwan) at 50 rpm and with a chamber wall temperature of 80 °C. The CBS and sulfur curatives were added in the second mixing stage on a two-roll mill at a temperature of 60 °C.

Cure behavior was evaluated at 160 °C using a moving die rheometer (MDR 3000 Basic from MonTech, Buchen, Germany) according to ASTM D6204. Planar tension (pure shear) test specimens were formed by curing the rubber in a mold, to give a testing geometry with dimensions of gauge height = 10 mm, width = 100 mm, and thickness = 1.5 mm. Specimens were cured in a heated press (LaBEcon 300 from Fontijne Presses, Delft, the Netherlands) at conditions given in Table 1.

Cured test specimens were aged for 720 hours (30 days) at temperatures of 25, 50, 70, and 90 °C in air ovens.

The rubber samples were tested at 25 °C with an Intrinsic Strength Analyzer (ISA™) manufactured by Coesfeld GmbH, Dortmund, Germany (Figs. 3 and 4), and operated with testing methodology developed by Endurica LLC, Findlay, Ohio, that is based on the approach of Lake and Yeoh [15]. In this method, shown schematically in Fig. 5, a planar tension test specimen, which is pre-cracked at one edge, is strained to each of several different strain levels in the range from 0 to 0.5 (0 to 50%). The specimen is held at each fixed strain and allowed to equilibrate for 10 minutes, after which the stress is determined from the normal force before initiating the cutting. A stress–strain curve is generated by combining the results from the different strain levels. After equilibration at each strain, a highly sharpened blade is brought into contact with the crack tip, and it is driven to slice the specimen at three constant, sequential rates that are decreasing in value, from 10 to 0.1 to 0.01 mm/min. The specialty blade is

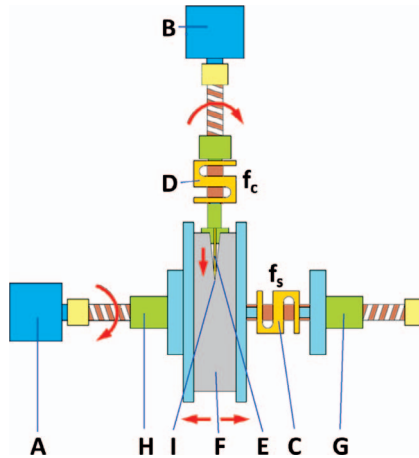


FIG. 4 — ISA measurement principle, where A, actuator of the stretching; B, actuator of cutting; C, loading cell of the stretching; D, loading cell of the cutting; E, razor blade; F, test specimen; G, clamping system of test specimen; H, clamping system of test specimen; I, razor blade tip. The measured stretching force is f_s and the measured cutting force is f_c .

produced by Lutz Blades (product reference number 0410.0100; length = 43 mm, width = 22.2 mm, and thickness = 0.10 mm). The steady state reaction force on the blade during cutting, f , is measured at each cutting rate for each strain level.

For an edge-cracked planar tension specimen under strain, with no blade applied, the tearing energy T is computed as the product of the strain energy density W and the unstrained section gauge height h .

$$T = Wh \quad (1)$$

The strain energy density W in the specimen is determined as a function of strain by numerically integrating the stress–strain curve.

During cutting by a blade, the moving force f required to maintain a constant rate of cutting does work, imparting an additional contribution to the total energy release rate driving the crack tip. This is called the cutting energy F , and its value is given by

$$F = f/t \quad (2)$$

where t is the thickness of the specimen [15].

Results and Discussion

Fatigue crack growth and tear strength properties involve a considerable extra energy contribution due to viscoelastic energy losses, thus preventing the

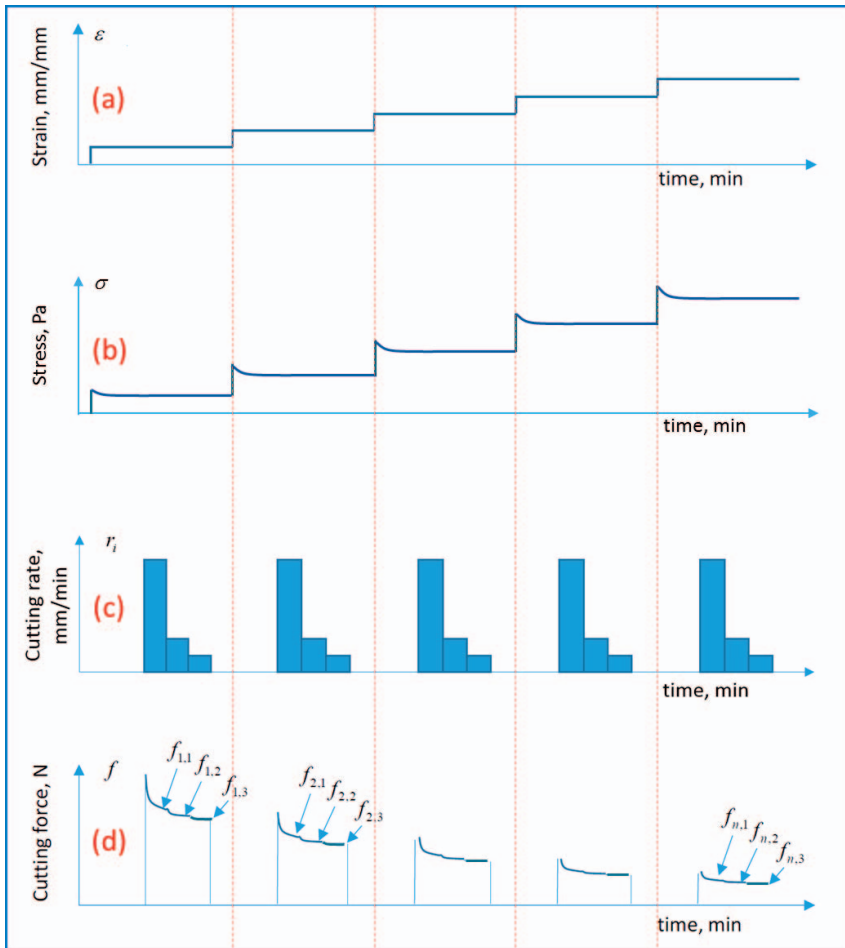


FIG. 5 — Testing protocol used for material evaluations with the ISA. (a) The crack is opened by stretching the specimen, (b) the stress is equilibrated, (c) then the blade is pushed into the open crack at three decreasing cutting speeds, and (d) the corresponding cutting forces are recorded. The process is repeated for other strain levels at increasing intervals.

effective characterization of molecular-level fracture strengths. A cutting approach was pioneered by Lake and Yeoh [15] to minimize crack tip dissipation in a cross-linked elastomer. The cutting and fatigue crack growth methods are contrasted in Fig. 6 with regard to the differing effects on the polymer network chains and related dissipation at the growing crack front.

When crack tip dissipation is sufficiently small, the intrinsic cutting energy $S_{0,c}$ for a strained planar tension specimen undergoing a cutting process may be written as the sum of the individual energy release rates for tearing and cutting

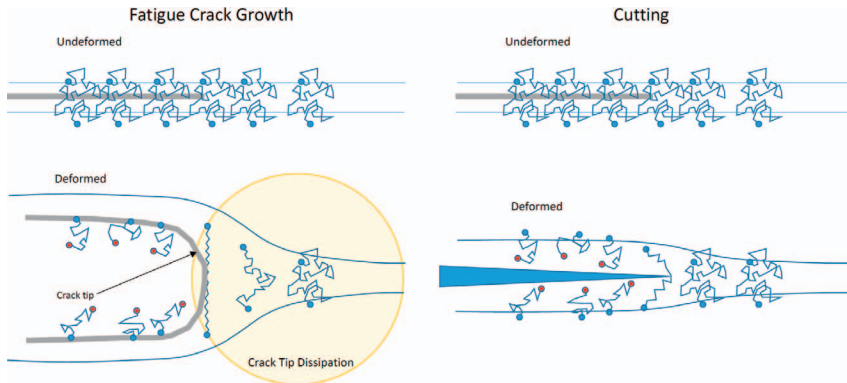


FIG. 6 — Illustration of the cutting approach to minimize crack tip dissipation in a cross-linked elastomer relative to typical fatigue crack growth and tear testing.

[15]:

$$S_{0,c} = T + F$$

which can be rearranged as

$$F = -T + S_{0,c} \quad (3)$$

$S_{0,c}$ is the intrinsic cutting energy that is to be determined via the measurements. T is the measured tearing energy, and F is the measured cutting energy. The intrinsic strength T_0 (endurance limit, fatigue threshold) is proportional to $S_{0,c}$, with a proportionality constant b that depends on the blade geometry and sharpness [15]:

$$T_0 = bS_{0,c} \quad (4)$$

The value of b can be evaluated from ISA testing of a control rubber material for which T_0 is known from separate fatigue crack growth testing near the threshold.

A schematic example of the way to assess $S_{0,c}$ from data collected using the ISA is given in Fig. 7. A line with slope of -1 on the cutting energy F versus tearing energy T plot—corresponding to Eq. (3)—that intersects with the data curve at the lowest possible point allows $S_{0,c}$ to be quantified from the intercepts of the line with the graph axes. In this manner, $S_{0,c}$ is determined from the test data for the rubber samples studied here using the lowest cutting rate of 0.01 mm/min. Representative data plots are provided in Figs. 8 and 9 for NR and the NR/BR (50/50) blend at two different aging temperatures (25 and 50 °C).

The control material was an unfilled SBR compound for which T_0 was reported to be 60 J/m² [15]. The ISA results for this rubber are shown in Fig. 10. The $S_{0,c}$ was determined to be 572 J/m², which gave $b = 0.105$ from Eq. (4).

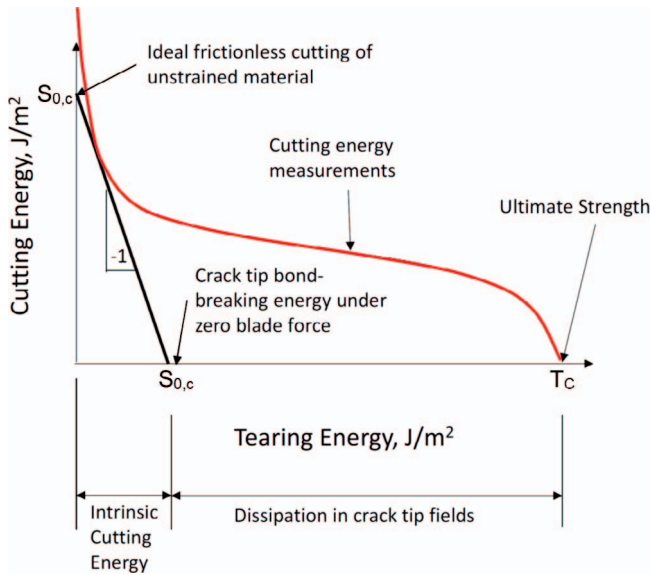


FIG. 7 — Method used to determine $S_{0,c}$ from F versus T data.

Quantifying this constant for the blade allowed the $S_{0,c}$ data from the ISA to be converted to T_0 values for the CB-filled NR, BR, and NR/BR blends.

The T_0 results are summarized in Fig. 11 for the materials as a function of the temperature where air aging was performed for 30 days prior to ISA testing at 25 °C. For the CB-filled pure elastomers and the two blends, the T_0 showed very large increases (100 to 300%) as the aging temperature was increased from 25 to 50 °C. This is a new discovery, and the possible origin of this substantial enhancement in intrinsic strength will be discussed later. Increasing the aging temperature further to 70 and 90 °C caused T_0 to progressively decrease from the maximum at 50 °C. This decrease in intrinsic strength with increasing temperatures from 50 to 90 °C can be understood if extra cross-linking introduced during thermal-oxidative aging is considered, as suggested from the aging-induced stiffening of the compounds (Fig. 12). It is generally known from both experimental data and theoretical considerations that the intrinsic strength scales with the molecular weight between cross-links (M_c) [2,22]:

$$T_0 \propto M_c^{1/2} \quad (5)$$

Given that M_c is inversely related to the density of cross-links, increases in cross-link density during aging should decrease T_0 .

The very significant improvement in intrinsic strength upon increasing the aging temperature from 25 to 50 °C—noted for all the rubber compositions studied—is striking and unexpected. The cutting was performed using the

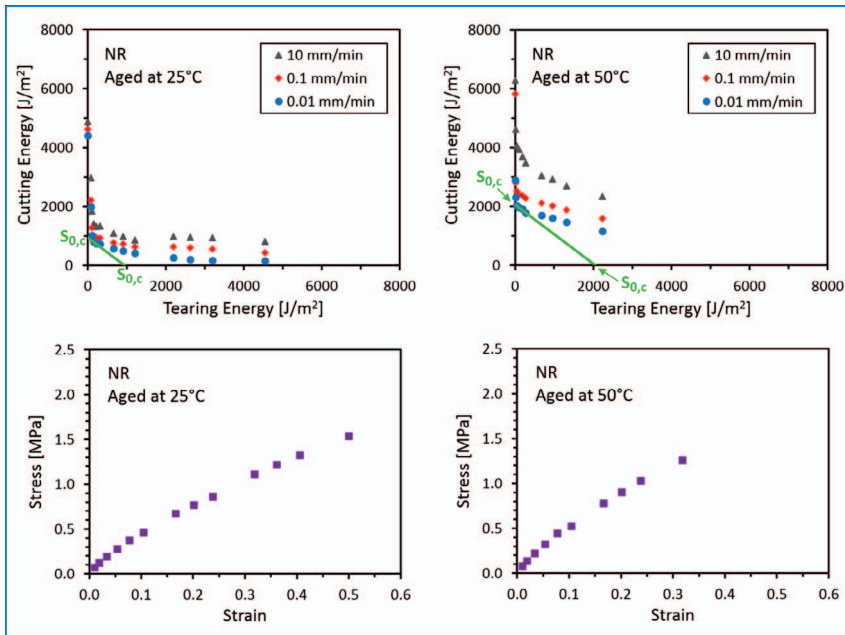


FIG. 8 — ISA results for the NR compound at the indicated aging temperatures of 25 °C (on left) and 50 °C (on right). The upper plots show the F versus T behaviors from which $S_{0,c}$ values are determined from the lowest cutting rate data, and the lower plots show stress–strain responses from which W and T are determined.

decreasing rate protocol with the intent of acquiring a rate-independent response to ensure that any significant viscoelastic dissipation influence on the cutting energy is eliminated. This was essentially achieved for the unfilled SBR material (Fig. 10), but all the CB-filled compounds (e.g., Figs. 8 and 9) produced cutting forces that still showed some rate dependence—possibly due to a localized Payne effect [23] near the blade cutting path. The rate dependence was not more pronounced after aging, however, so any filler network strengthening, akin to filler flocculation [24–26], cannot explain the results.

A notable finding is that aging for 30 days at 50 and 70 °C produces rather substantial positive deviations of T_0 from rule-of-mixtures additivity for both NR/BR blend compositions, with greater impact observed for aging at 50 °C compared with 70 °C. This is clearly evident in Fig. 13. This means that the durability performance of a CB-filled NR/BR blend is projected to become better than the expected contributions from NR and BR as time progresses during use in a tire component, since normal operating temperatures of tire sidewall compounds, for example, overlap this 50 to 70 °C temperature range.

The multi-scale and complex nature of the various structural characteristics of the CB-reinforced immiscible blend of NR and BR (Fig. 14) [27,28] makes it

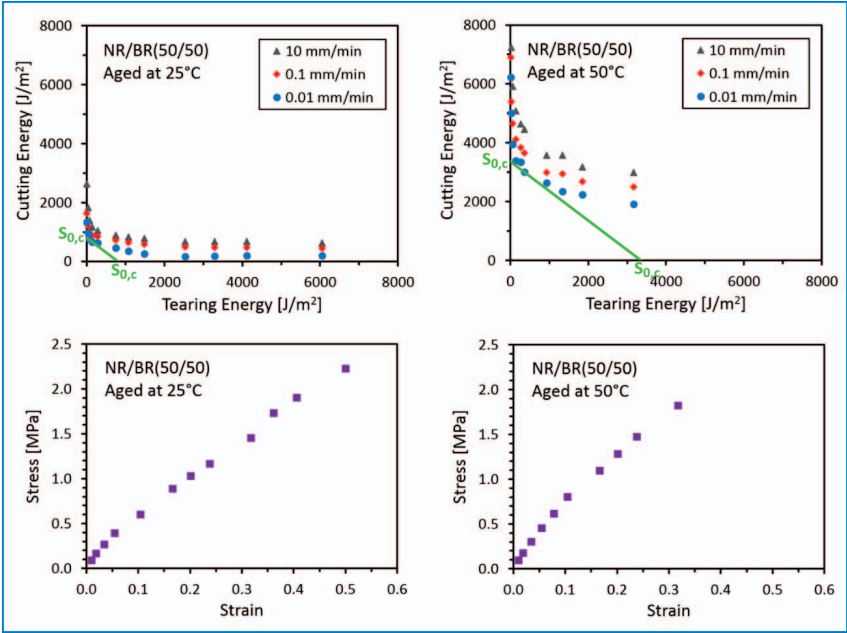


FIG. 9 — ISA results for the NR/BR(50/50) compound at the indicated aging temperatures of 25 °C (on left) and 50 °C (on right). The upper plots show the F versus T behaviors from which $S_{0,c}$ values are determined from the lowest cutting rate data, and the lower plots show stress–strain responses from which W and T are determined.

difficult to rationalize the observed dependence of intrinsic strength on blend composition and aging temperature. Thermal annealing of the blends may allow for additional interpenetration and/or co-cross-linking of dissimilar polymer chains at the NR–BR phase boundaries. Annealing can also lead to the

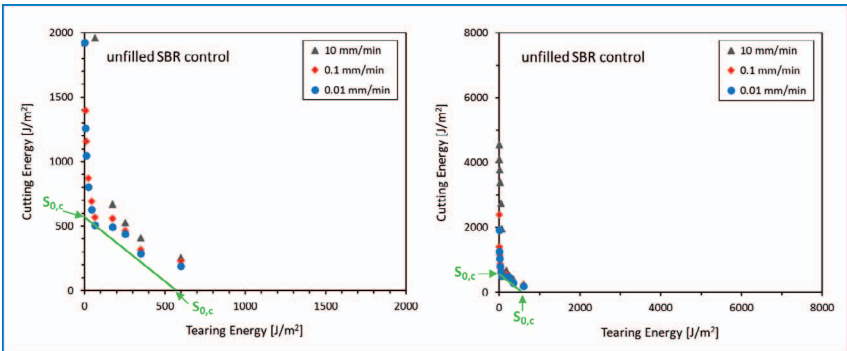


FIG. 10 — ISA results for the unfilled control SBR compound. The F versus T plot on the right has expanded axes scales to allow comparison with Figs. 8 and 9.

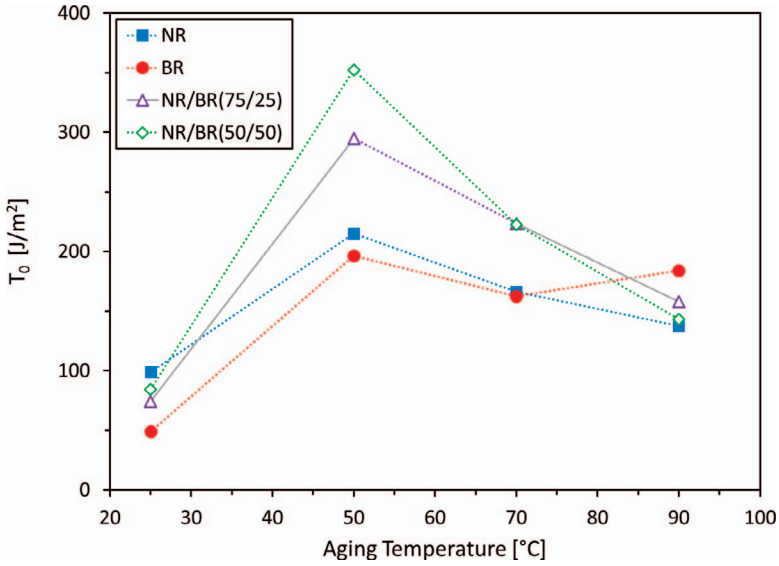


FIG. 11 — Aging temperature dependence of T_0 for the rubber compounds. The rubber specimens were aged for 30 days at the indicated temperatures before testing at 25 °C.

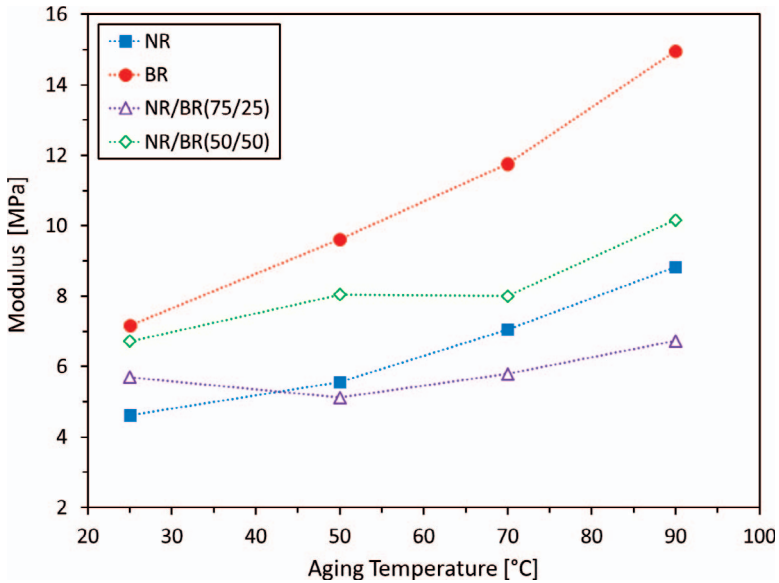


FIG. 12 — Small strain (0.05) modulus in planar extension versus aging temperature for the rubber compounds. The rubber specimens were aged for 30 days at the indicated temperatures before testing at 25 °C.

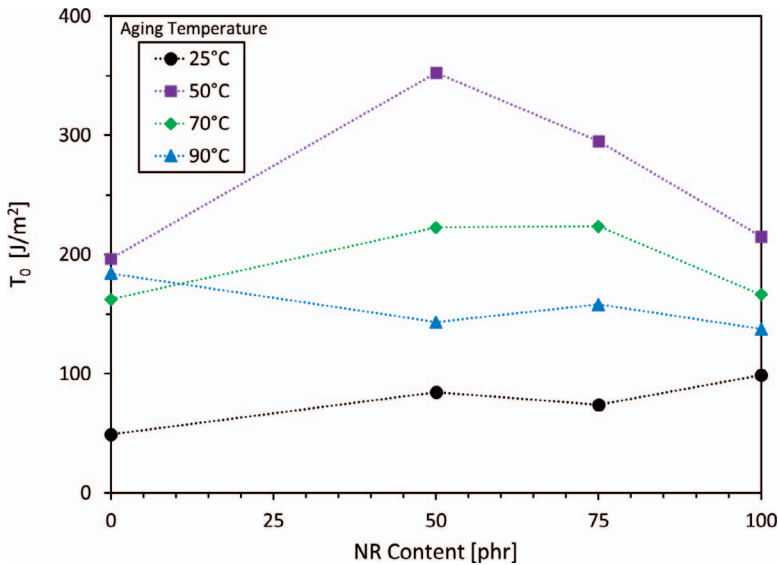


FIG. 13 — Effect of blend composition on T_0 after aging for 30 days at the indicated temperatures before testing at 25 °C.

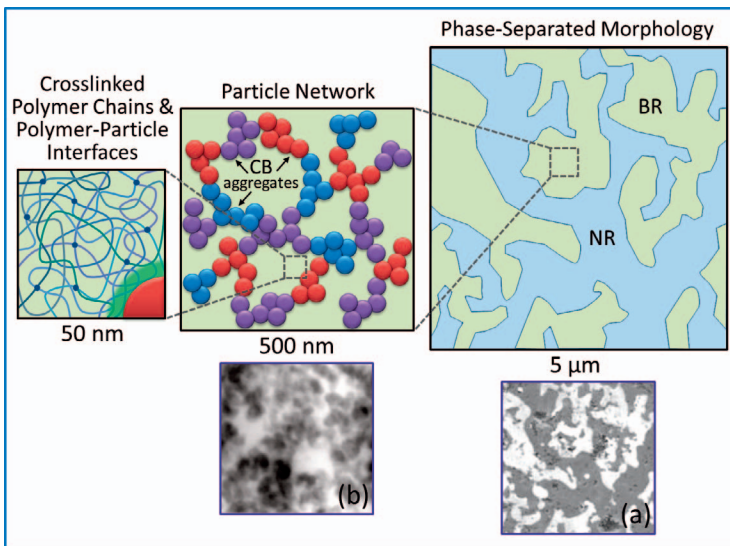


FIG. 14 — Structural features and their approximate length scales in a carbon black reinforced NR/BR blend; (a) AFM phase contrast image ($5 \mu\text{m} \times 5 \mu\text{m}$) for an unfilled NR/BR(60/40) blend, adapted from Inoue et al. [27]; (b) TEM image ($500 \text{ nm} \times 500 \text{ nm}$) for BR filled with 23 vol% of N339 CB, adapted from Robertson and Rackaitis [28].

development of stronger bound rubber layers at the polymer–filler interfaces and/or augmentations of the filler networks via rotations/movements of particles across small distances, but these can presumably happen in both neat elastomers and blends alike. Future research studies are needed to confirm the results and uncover the key structural cause for the development of unexpected intrinsic strength enhancements for the blends relative to the pure polymer contributions, only after aging at relatively modest temperatures.

Final Comments

Use of the instrumented cutting method enabled the effects of polymer blend composition and aging temperature on intrinsic strength to be investigated for a CB-filled NR/BR blend system. Aging for 30 days at 50 and 70 °C gives very significant positive increases in T_0 for the blends above composition-averaged contributions from the NR and BR. This temperature range is very relevant to tire applications, and these new intrinsic strength findings may therefore help explain why CB-reinforced NR/BR blends are successfully employed as highly durable compounds in tire sidewalls and in some TBR treads.

The experimental procedure on the ISA executes in a few hours compared with several months for fatigue crack growth testing near the endurance limit, and it provides insight into molecular-level parameters thought to govern long-term durability of a rubber compound in service. Fundamental studies are needed to establish how intrinsic strength is influenced by (1) reinforcing particle type and concentration; (2) nature of polymer–filler interactions promoted by coupling agents, functionalized polymers, and additives; and (3) other leading-edge materials and compounding philosophies being developed for tire compounds.

References

- [1] Lake, G. J. and Yeoh, O. H., “Effect of Crack Tip Sharpness on the Strength of Vulcanized Rubbers,” *Journal of Polymer Science: Part B: Polymer Physics*, Vol. 25, 1987, pp. 1157–1190.
- [2] Bhowmick, A. K., “Threshold Fracture of Elastomers,” *Journal of Macromolecular Science, Part C: Polymer Reviews*, Vol. 28, 1988, pp. 339–370.
- [3] Lake, G. J. and Thomas, A. G., “The Strength of Highly Elastic Materials,” *Proceedings of the Royal Society of London A*, Vol. 300, 1967, pp. 108–119.
- [4] Gent, A. N. and Mars, W. V., “Strength of Elastomers,” *Science and Technology of Rubber*, 4th ed., Chapter 10, 2013, pp. 473–516.
- [5] Lake, G. J. and Lindley, P. B., “Mechanical Fatigue Limit for Rubber,” *Rubber Chemistry and Technology*, Vol. 39, 1966, pp. 348–364.

- [6] Andrews, E. H., "Rupture Propagation in Hysterical Materials: Stress at a Notch," *Journal of the Mechanics and Physics of Solids*, Vol. 11, 1963, pp. 231–242.
- [7] Mars, W. V., Kipscholl, C., and Stoček, R., "Intrinsic Strength Analyzer Based on the Cutting Method," *Fall 190th Technical Meeting*, Rubber Division of the American Chemical Society, Inc., Pittsburgh, PA, October 10–13, 2016.
- [8] Mars, W. V., "Fatigue Life Prediction for Elastomeric Structures," *Rubber Chemistry and Technology*, Vol. 80, 2007, pp. 481–503.
- [9] Stoček, R., Horst, T., and Reincke, K., "Tearing Energy as Fracture Mechanical Quantity for Elastomers," *Advances in Polymer Science*, Vol. 275, 2016, pp. 361–398.
- [10] Mars, W. V. and Fatemi, A., "Factors That Affect the Fatigue Life of Rubber: A Literature Survey," *Rubber Chemistry and Technology*, Vol. 77, 2004, pp. 391–412.
- [11] Harbour, R. J., Fatemi, A., and Mars, W. V., "The Effect of a Dwell Period on Fatigue Crack Growth Rates in Filled SBR and NR," *Rubber Chemistry and Technology*, Vol. 80, 2007, pp. 838–853.
- [12] Andreini, G., Straffi, P., Cotugno, S., Gallone, G., and Polacco, G., "Crack Growth Behavior of Styrene-Butadiene Rubber, Natural Rubber, and Polybutadiene Rubber Compounds: Comparison of Pure-Shear versus Strip Tensile Test," *Rubber Chemistry and Technology*, Vol. 86, 2013, pp. 132–145.
- [13] Stadlbauer, F., Koch, T., Planitzer, F., Fidi, W., and Archodoulaki, V.-M., "Setup Evaluation of Fatigue Crack Growth in Rubber: Pure Shear Sample Geometries Testing in Tension-Compression Mode," *Polymer Testing*, Vol. 32, 2013, pp. 1045–1051.
- [14] Stadlbauer, F., Koch, T., Archodoulaki, V.-M., Planitzer, F., Fidi, W., and Holzner, A., "Influence of Experimental Parameters on Fatigue Crack Growth and Heat Build-Up in Rubber," *Materials*, Vol. 6, 2013, pp. 5502–5516.
- [15] Lake, G. J. and Yeoh, O. H., "Measurement of Rubber Cutting Resistance in the Absence of Friction," *International Journal of Fracture*, Vol. 14, 1978, pp. 509–526.
- [16] Hess, W. M., Scott, C. E., and Callan, J. E., "Carbon Black Distribution in Elastomer Blends," *Rubber Chemistry and Technology*, Vol. 40, 1967, pp. 371–384.
- [17] Hamed, G. R., Kim, H. J., and Gent, A. N., "Cut Growth in Vulcanizates of Natural Rubber, cis-Polybutadiene, and a 50/50 Blend during Single and Repeated Extension," *Rubber Chemistry and Technology*, Vol. 69, 1996, pp. 807–818.
- [18] Lee, M.-P. and Moet, A., "Analysis of Fatigue Crack Propagation in NR/BR Rubber Blend," *Rubber Chemistry and Technology*, Vol. 66, 1993, pp. 304–316.
- [19] Kim, H. J. and Hamed, G. R., "On the Reason that Passenger Tire Sidewalls are Based on Blends of Natural Rubber and cis-Polybutadiene," *Rubber Chemistry and Technology*, Vol. 73, 2000, pp. 743–752.
- [20] Wunde, M. and Klüppel, M., "Influence of Phase Morphology and Filler Distribution in NR/BR and NR/SBR Blends on Fracture Mechanical Properties," *Rubber Chemistry and Technology*, Vol. 89, 2016, pp. 588–607.
- [21] Ghosh, P., Stoček, R., Gehde, M., Mukhopadhyay, R., and Krishnakumar, R., "Investigation of Fatigue Crack Growth Characteristics of NR/BR Blend Based Tyre Tread Compounds," *International Journal of Fracture*, Vol. 188, 2014, pp. 9–21.
- [22] Gent, A. N. and Tobias, R. H., "Threshold Tear Strength of Elastomers," *Journal of Polymer Science: Polymer Physics Edition*, Vol. 20, 1982, pp. 2051–2058.
- [23] Payne, A. R., "The Dynamic Properties of Carbon Black-Loaded Natural Rubber Vulcanizates," *Journal of Applied Polymer Science*, Vol. 6, 1962, pp. 57–62.

- [24] Bohm, G. A., Tomaszewski, W., Cole, W., and Hogan, T., "Furthering the Understanding of the Non Linear Response of Filler Reinforced Elastomers," *Polymer*, Vol. 51, 2010, pp. 2057–2068.
- [25] Tunncliffe, L. B., Kadlcak, J., Morris, M. D., Shi, Y., Thomas, A. G., and Busfield, J. J. C., "Flocculation and Viscoelastic Behaviour in Carbon Black-Filled Natural Rubber," *Macromolecular Materials and Engineering*, Vol. 299, 2014, pp. 1474–1483.
- [26] Robertson, C. G., Lin, C. J., Bogoslovov, R. B., Rackaitis, M., Sadhukhan, P., Quinn, J. D., and Roland, C. M., "Flocculation, Reinforcement, and Glass Transition Effects in Silica-Filled Styrene-Butadiene Rubber," *Rubber Chemistry and Technology*, Vol. 84, 2011, pp. 507–519.
- [27] Inoue, Y., Iwasa, M., and Yoshida, H., "Variable Temperature AFM Observation of Phase Separation in NR/BR Blend," *Netsu Sokutei*, Vol. 39, 2012, pp. 41–46.
- [28] Robertson, C. G. and Rackaitis, M., "Further Consideration of Viscoelastic Two Glass Transition Behavior of Nanoparticle-Filled Polymers," *Macromolecules*, Vol. 44, 2011, pp. 1177–1181.